# Statistical considerations for multiband resting-state fMRI studies

Benjamin Risk

Department of Biostatistics & Bioinformatics, Emory University
thebrisklab

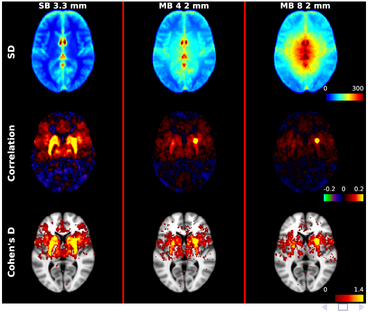

# Collaborators

Collaborators on multiband: Raphiel Murden (Emory), Deqiang Qiu (Emory), Junjie Wu (Emory), Zhengwu Zhang (UNC), Vankee Lin (Stanford), Arun Venkataraman (University of Rochester), Mary Beth Nebel (JHU), Dan Rowe (Marquette), Mary Kociuba (Amazon).

Also thanks to other collaborators in fMRI: Emory Center for Biomedical Imaging Statistics, Ying Guo, Suprateek Kundu, Irina Gaynanova.

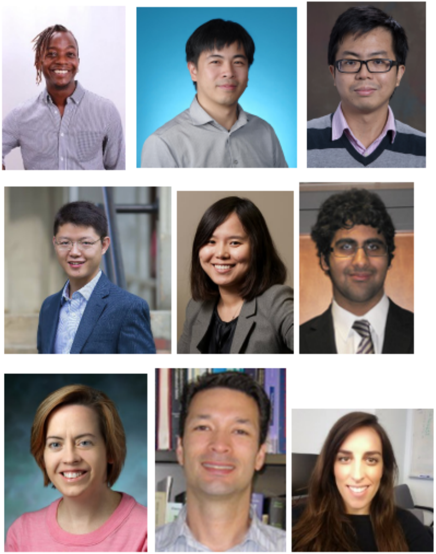

# Part 1: Overview of Multiband

# What is multiband?

- Multiband is an acquisition method commonly used in fMRI and dMRI studies Setsompop et al. (2012).
- Also called simultaneous multislice.
- HCP, UK Biobank, ABCD, ADNI 3 Advanced.
- Method to acquire images faster: higher temporal resolution in fMRI.
- Higher temporal resolution allows higher spatial resolution (e.g., 2 mm), which is needed for cortical surface analysis.

# Multiband acquisition

- 2D EPI used for most fMRI and dMRI.
- Instead of one slice at-a-time, collect multiple.
- Multiple slices collected in a “single image,” separated afterwards.
- Separation leads to noise amplification (Setsompop et al., 2012).

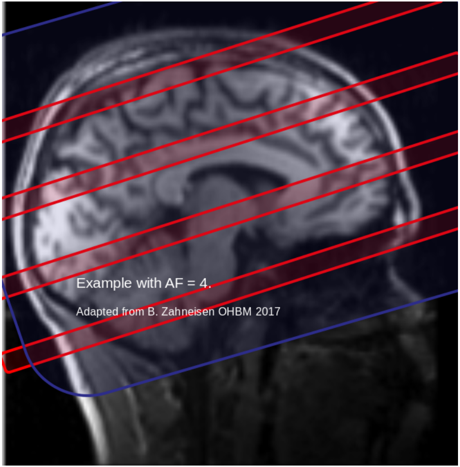

# Lower correlations in multiband

https://www.mail-archive.com/hcp-users@humanconnectome.org/msg06484.html

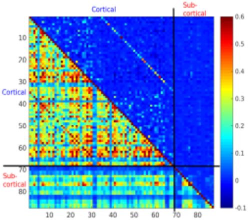


```
> On Mon, Jul 9, 2018 at 10:48 PM, Glasser, Matthew <glass...@wustl.edu>
> wrote:
>
>> There is more unstructured noise in HCP data because of small voxel size
>> and fast TR.  Basically that means the ratio between the neural signal and
>> the random noise is lower and that leads to lower correlation coefficients.
>>
>>
>> Peace,
>>
>> Matt.
```

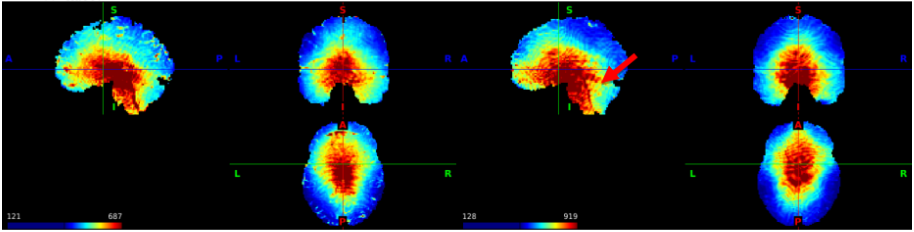

# Lower correlations and noise amplification

Consider a simplified model.

- Define the signal between two locations:

$$\begin{bmatrix} x_{ivt} \\ x_{iv't} \end{bmatrix} \sim \left( \begin{bmatrix} \mu_v \\ \mu_{v'} \end{bmatrix}, \begin{bmatrix} \sigma_v^2 & \psi_{vv'} \\ \psi_{vv'} & \sigma_{v'}^2 \end{bmatrix} \right).$$

- In multiband acquisitions, there is noise amplification:

$$y_{iavt} = x_{ivt} + \epsilon_{iavt},\ \epsilon_{iavt} \sim (0, \eta_{av}^2)$$

- Then in areas with greater noise amplification, correlations decrease:

$$\text{Corr}(y_{iavt}, y_{iav't}) = \frac{\psi_{vv'}}{\sqrt{\sigma_v^2 + \eta_{av}^2}\sqrt{\sigma_{v'}^2 + \eta_{av'}^2}},$$

# What is the impact on power?

Fisher z-transform correlations:

$$z_{iavv'} \overset{iid}{\sim} \mathcal{N}(z_{avv'}, \nu_{avv'}^2),$$

$$\Phi\left(\sqrt{N}\frac{z_{avv'}}{\nu_{avv'}} - c_{1-\alpha}\right).$$

- In the absence of autocorrelation, $\nu_{avv'}^2 \approx 1/T_a$.
- For $N$ independent subjects, $\mathrm{Var}\sum_{i=1}^{N} z_{iavv'}/N \approx 1/(NT_a)$.
- In general, $\nu_{avv'}^2 > 1/T_a$ in the presence of positive autocorrelation.
- An increase in the MB factor may simultaneously *decrease* $z_{avv'}$ and *decrease* $\nu_{avv'}$.

# Part 2: The Emory Multiband Study

# The Emory Multiband Study

- 32 subjects.
- Evaluate 9 acquisitions. All runs approximately 6 minutes.
- 9p preprocessing: 6 parameters from rigid-body motion correction, global signal, white matter, and cerebrospinal fluid.
- Bandpass: 0.009 - 0.08 Hz. Discrete cosine basis in the time-domain bandpass filtering via AFNI's 3dTproject
- Note: simultaneous bandpass and nuisance regression (Lindquist et al., 2019).

| MB | 1 | 1 | 2 | 3 | 4 | 6 | 8 | 9 | 12 |
|---|---|---|---|---|---|---|---|---|---|
| TR (ms) | 3000 | 5670 | 2850 | 1910 | 1440 | 962 | 736 | 675 | 512 |
| Voxel Size | 3.3 | 2 | 2 | 2 | 2 | 2 | 2 | 2 | 2 |
| FA | 81 | 88 | 80 | 72 | 65 | 57 | 51 | 48 | 43 |
| N vol | 114 | 62 | 121 | 182 | 241 | 353 | 464 | 505 | 668 |
| df lost in bp | 65 | 13 | 72 | 133 | 192 | 306 | 415 | 458 | 619 |
| df after 9p+bp | 37 | 37 | 37 | 37 | 37 | 35 | 37 | 35 | 37 |

# Noise Amplification

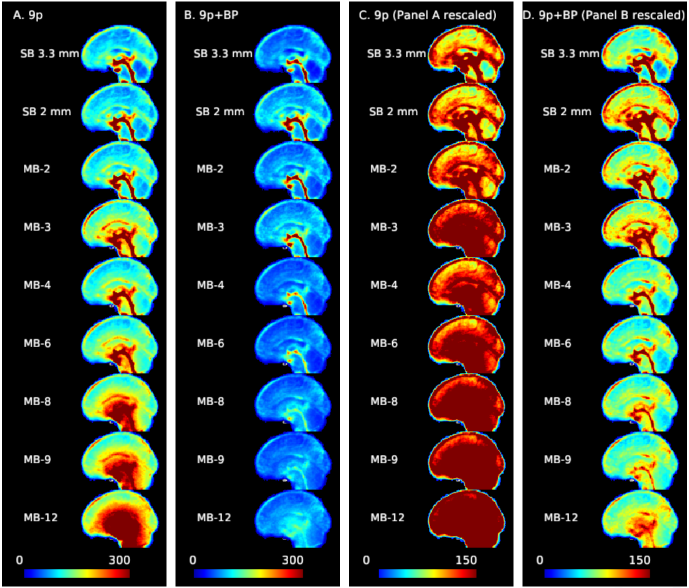

# Impacts on putamen connectivity

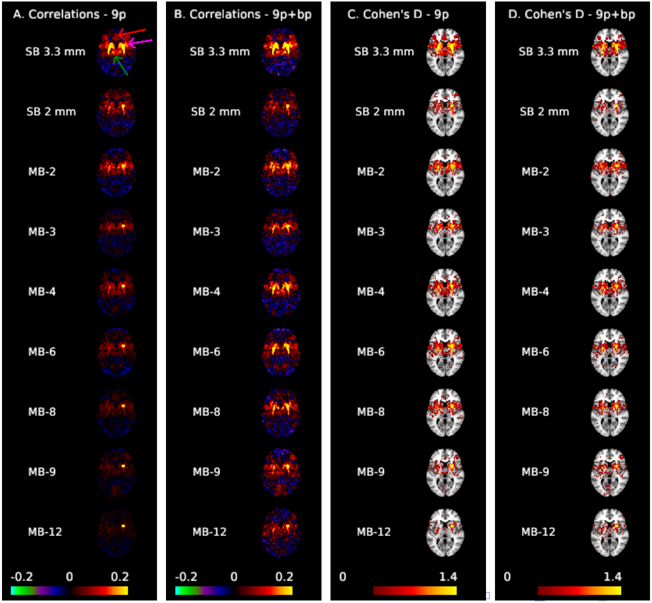

# Motor-thalamic connectivity

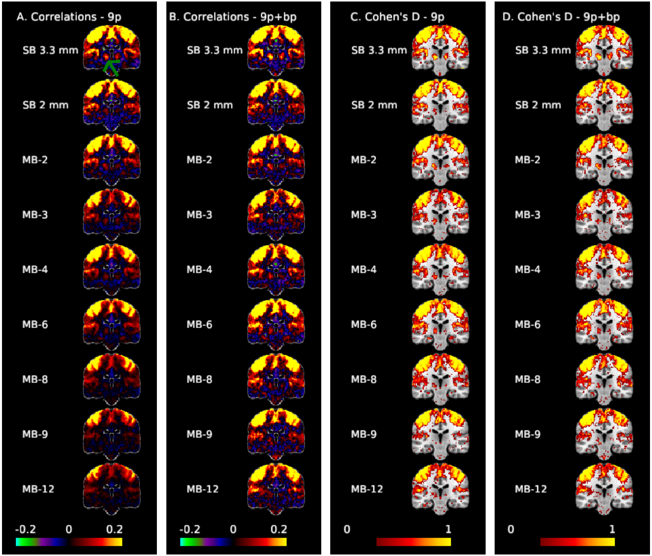

# Conclusions from seed maps

- Correlations and effect sizes are much larger at SB 3.3 mm in the putamen as well as motor-thalamic.
- MB 2 and 4 do well among 2 mm.
- Temporal filtering increases correlations, reduces spatial biases in correlations
- In these seed maps, temporal filtering has comparatively minor impacts on power.

# Correlation matrices

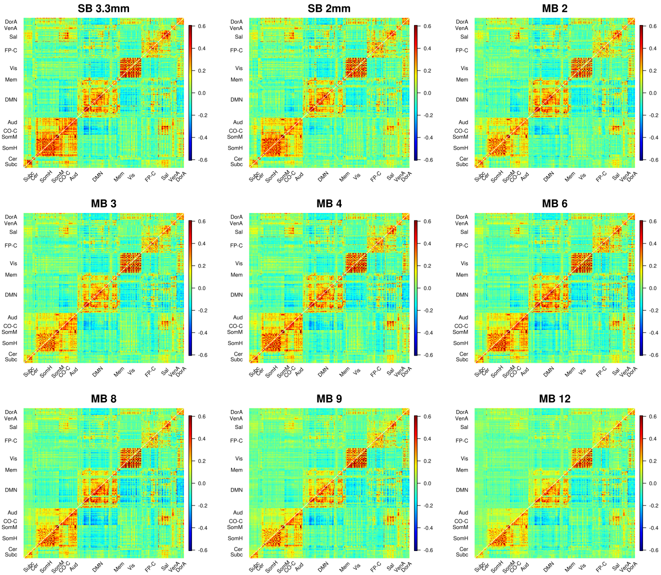

# Selected edges

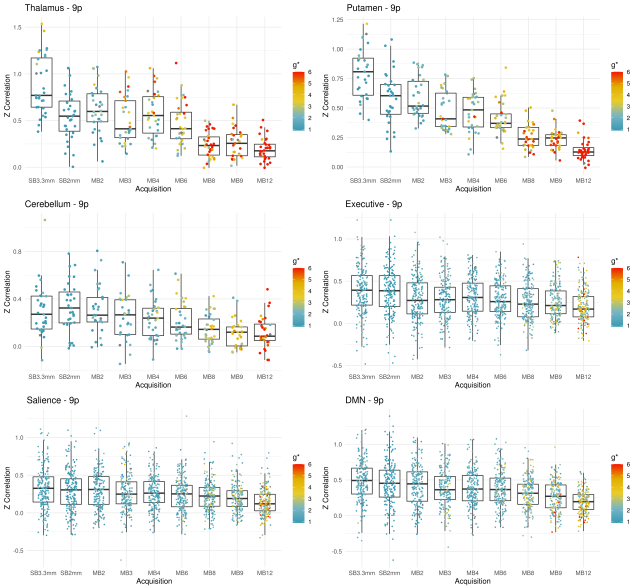

# Selected edges: with temporal filtering (bandpass)

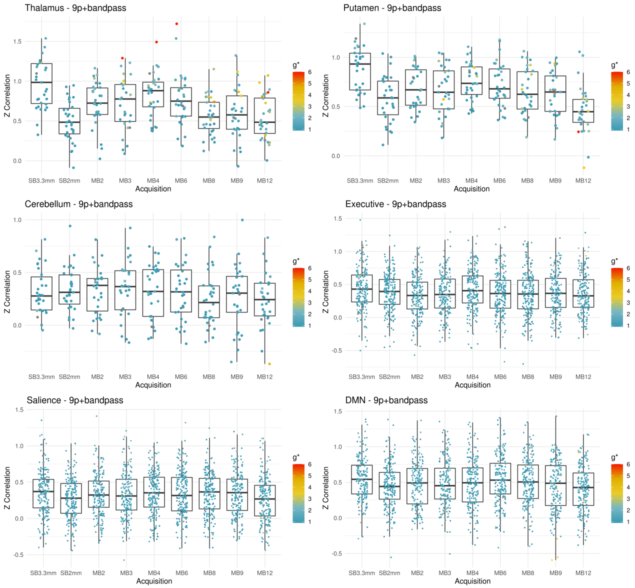

# Effect sizes

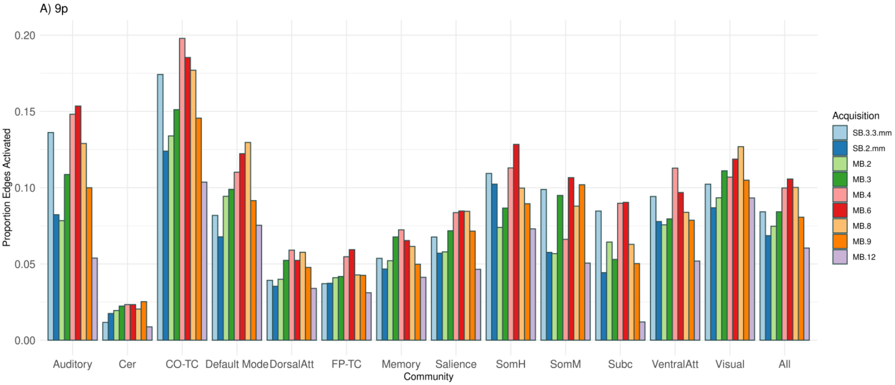

# Effect sizes: perm tests

| | SB 3.3 mm | SB 2 mm | MB 2 | MB 3 |
|---|---|---|---|---|
| Auditory | 0.005 p=0.765 | **-0.042 p=0.008** | -0.041 p=0.022 | -0.01 p=0.474 |
| Cerebellum | -0.007 p=0.171 | 0.001 p=0.71 | -0.002 p=0.55 | -0.001 p=0.838 |
| CO-Task Ctrl | 0.001 p=0.966 | **-0.051 p=0** | -0.039 p=0.048 | -0.016 p=0.442 |
| Default Mode | **-0.043 p=0.001** | **-0.059 p=0** | -0.033 p=0.016 | -0.025 p=0.07 |
| Dorsal Att | -0.014 p=0.048 | **-0.023 p=0** | -0.01 p=0.066 | -0.003 p=0.618 |
| FP-Task Ctrl | -0.007 p=0.244 | -0.005 p=0.234 | -0.005 p=0.385 | -0.002 p=0.748 |
| Memory | -0.003 p=0.772 | -0.011 p=0.364 | -0.003 p=0.747 | 0.008 p=0.476 |
| Salience | -0.014 p=0.067 | **-0.025 p=0** | **-0.027 p=0** | -0.014 p=0.082 |
| Som-Hand | 0.011 p=0.513 | 0.005 p=0.793 | -0.02 p=0.096 | -0.004 p=0.74 |
| Som-Mouth | 0.009 p=0.684 | -0.027 p=0.086 | -0.027 p=0.082 | 0.009 p=0.619 |
| Subcortical | 0.023 p=0.097 | -0.018 p=0.022 | 0.007 p=0.473 | 0.001 p=0.904 |
| Ventral Att | 0.01 p=0.384 | -0.003 p=0.78 | -0.005 p=0.589 | -0.003 p=0.783 |
| Visual | -0.023 p=0.012 | **-0.039 p=0.002** | **-0.035 p=0.001** | -0.018 p=0.227 |
| All | -0.014 p=0.053 | **-0.029 p=0** | **-0.022 p=0.002** | -0.011 p=0.149 |
| | **MB 4** | **MB 6** | **MB 9** | **MB 12** |
| Auditory | 0.019 p=0.362 | 0.025 p=0.178 | -0.029 p=0.072 | **-0.075 p=0** |
| Cerebellum | 0.008 p=0.159 | 0.003 p=0.728 | 0.007 p=0.324 | -0.012 p=0.055 |
| CO-Task Ctrl | 0.023 p=0.381 | 0.008 p=0.708 | -0.026 p=0.208 | **-0.073 p=0.001** |
| Default Mode | -0.019 p=0.205 | -0.007 p=0.584 | **-0.03 p=0.008** | **-0.054 p=0** |
| Dorsal Att | 0.004 p=0.535 | -0.005 p=0.528 | -0.013 p=0.036 | **-0.024 p=0.004** |
| FP-Task Ctrl | 0.011 p=0.062 | 0.017 p=0.012 | 0 p=0.94 | -0.012 p=0.025 |
| Memory | 0.008 p=0.546 | 0.004 p=0.766 | -0.014 p=0.118 | -0.02 p=0.065 |
| Salience | -0.003 p=0.724 | 0 p=0.972 | -0.018 p=0.018 | **-0.038 p=0** |
| Som-Hand | 0.016 p=0.34 | 0.029 p=0.143 | -0.013 p=0.297 | -0.027 p=0.092 |
| Som-Mouth | -0.017 p=0.258 | 0.019 p=0.406 | 0.007 p=0.665 | -0.037 p=0.037 |
| Subcortical | 0.026 p=0.06 | 0.028 p=0.07 | -0.009 p=0.41 | **-0.051 p=0** |
| Ventral Att | 0.026 p=0.039 | 0.013 p=0.337 | -0.005 p=0.632 | **-0.032 p=0.001** |
| Visual | -0.019 p=0.2 | -0.008 p=0.479 | -0.024 p=0.057 | **-0.034 p=0.009** |
| All | 0.001 p=0.952 | 0.006 p=0.458 | **-0.018 p=0.004** | **-0.04 p=0** |

Table S.2: Difference between the proportion of significant edges in the indicated acquisition versus MB 8 in 9p preprocessing, where negative values indicate greater activation in MB 8. Proportions for a given community include all edges in which at least one node belonged to the community. P-values are based on 10,000 permutations and are not corrected for multiple comparisons. Bold indicates $p < 0.01$.

# Effect sizes with temporal filtering

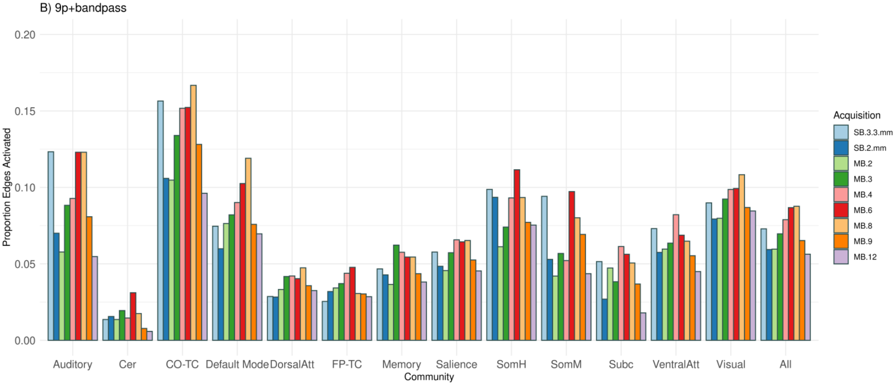

# Temporal filtering: not clear if good or bad

| | SB 3.3 mm | SB 2 mm | MB 2 | MB 3 | MB 4 |
|---|---|---|---|---|---|
| Auditory | 0.019 p=0.02 | **0.013 p=0.008** | **0.021 p=0.002** | 0.019 p=0.017 | **0.051 p=0** |
| Cerebellum | -0.001 p=0.62 | 0 p=0.861 | 0.003 p=0.218 | 0.002 p=0.526 | **0.009 p=0.008** |
| CO-Task Ctrl | **0.021 p=0.002** | 0.013 p=0.023 | **0.023 p=0.008** | 0.018 p=0.023 | **0.047 p=0.003** |
| Default Mode | 0.009 p=0.069 | 0.008 p=0.022 | **0.016 p=0.006** | 0.014 p=0.031 | **0.021 p=0.002** |
| Dorsal Att | **0.01 p=0** | 0.005 p=0.017 | 0.007 p=0.063 | 0.008 p=0.064 | **0.017 p=0** |
| FP-Task Ctrl | **0.01 p=0.001** | 0.007 p=0.017 | 0.008 p=0.021 | 0.006 p=0.041 | **0.01 p=0.003** |
| Memory | 0.009 p=0.033 | 0.004 p=0.194 | 0.01 p=0.02 | -0.001 p=0.897 | 0.009 p=0.292 |
| Salience | **0.013 p=0.008** | **0.011 p=0.001** | **0.013 p=0** | **0.015 p=0.003** | **0.02 p=0.001** |
| Som-Hand | 0.008 p=0.141 | 0.011 p=0.014 | 0.009 p=0.047 | **0.014 p=0.002** | 0.019 p=0.042 |
| Som-Mouth | 0.009 p=0.328 | 0.005 p=0.259 | 0.012 p=0.043 | **0.033 p=0** | 0.013 p=0.035 |
| Subcortical | **0.029 p=0** | **0.018 p=0** | **0.017 p=0** | **0.016 p=0.001** | **0.033 p=0** |
| Ventral Att | **0.018 p=0.001** | **0.019 p=0** | 0.012 p=0.04 | **0.015 p=0.004** | **0.031 p=0** |
| Visual | **0.013 p=0.006** | **0.009 p=0.004** | **0.013 p=0.002** | **0.015 p=0.004** | 0.01 p=0.078 |
| All | **0.012 p=0** | **0.009 p=0** | **0.013 p=0** | **0.013 p=0** | **0.021 p=0** |

| | MB 6 | MB 8 | MB 9 | MB 12 |
|---|---|---|---|---|
| Auditory | **0.031 p=0.002** | 0.006 p=0.691 | 0.019 p=0.05 | -0.001 p=0.893 |
| Cerebellum | -0.008 p=0.158 | 0.003 p=0.517 | 0.013 p=0.012 | 0.003 p=0.298 |
| CO-Task Ctrl | **0.033 p=0.001** | 0.01 p=0.58 | 0.019 p=0.19 | 0.008 p=0.517 |
| Default Mode | **0.02 p=0.002** | 0.011 p=0.282 | 0.015 p=0.015 | 0.006 p=0.322 |
| Dorsal Att | **0.012 p=0.002** | 0.01 p=0.046 | 0.009 p=0.079 | 0.001 p=0.672 |
| FP-Task Ctrl | 0.012 p=0.017 | **0.012 p=0.007** | **0.011 p=0.009** | 0.003 p=0.427 |
| Memory | 0.011 p=0.199 | 0.007 p=0.356 | 0.005 p=0.337 | 0.003 p=0.667 |
| Salience | **0.02 p=0** | **0.019 p=0** | **0.018 p=0** | 0.001 p=0.792 |
| Som-Hand | 0.017 p=0.039 | 0.006 p=0.547 | 0.013 p=0.072 | -0.002 p=0.811 |
| Som-Mouth | 0.009 p=0.427 | 0.008 p=0.52 | **0.033 p=0.002** | 0.007 p=0.371 |
| Subcortical | **0.034 p=0** | 0.012 p=0.09 | 0.011 p=0.063 | -0.006 p=0.103 |
| Ventral Att | **0.028 p=0** | **0.019 p=0.001** | **0.017 p=0** | 0.007 p=0.186 |
| Visual | **0.019 p=0.001** | **0.019 p=0.009** | **0.015 p=0.007** | 0.009 p=0.158 |
| All | **0.019 p=0** | 0.013 p=0.019 | **0.014 p=0** | 0.004 p=0.263 |

Table S.5: Difference in proportion of significant correlations between 9p and 9p+bandpass. Positive values indicate a higher proportion in 9p. Proportions for a given community include all edges in which at least one node belonged to the community. P-values are based on 10,000 permutations and are not corrected for multiple comparisons. Bold indicates $p < 0.01$. Overall, there are more significant edges in 9p. Bold indicates $p < 0.01$.

# Highlights

1. Compared single-band 3.3 mm, 2 mm and multiband factors 2, 3, 4, 6, 8, 9, 12 at 2 mm
2. Multiband noise amplification creates spatial biases in rs-fMRI correlations
3. Temporal filtering reduces spatial biases but decreases effect sizes
4. Single-band 3.3 mm recommended for seed-based analyses involving subcortical regions
5. Multiband 4 is a good choice for whole-brain analyses with 2 mm isotropic voxels

# Part 3: Overview of Diffusion MRI in Older Adults

# Multiband Impacts in Older Adults

- dMRI: white matter integrity. Estimate streamlines (tracts) that are a proxy of the "wires" in the brain.
- Ideal acquisition: high reliability with low acquisition time.
- Balance noise amplification with motion reduction.
- $2 \times 2 \times 2$ mm$^3$ resolution, b-values: 14 interspersed $b = 0$, 26 $b = 1000$, and 102 $b = 2000$.
- Data acquisition in progress: 6 young, 20 older healthy, and 20 with mild cognitive impairment scanned at the University of Rochester.
- To do: 2 scanning sessions per participant to assess reliability.
- Preliminary results presented here.

| Slice Acc. (S) (same as MB) | Phase Acc. (P) | TE/TR (ms) | Acquisition Time (min:sec) |
|---|---|---|---|
| S1 | P1 | 82/9190 | 21:28 |
| S3 | P1 | 93/3378 | 8:10 |
| S3 | P2 | 82.2/2740 | 7:05 |
| S6 | P1 | 93/1723 | 4:17 |
| S6 | P2 | 82.2/1404 | 3:56 |

# Scan Quality: Preliminary Results

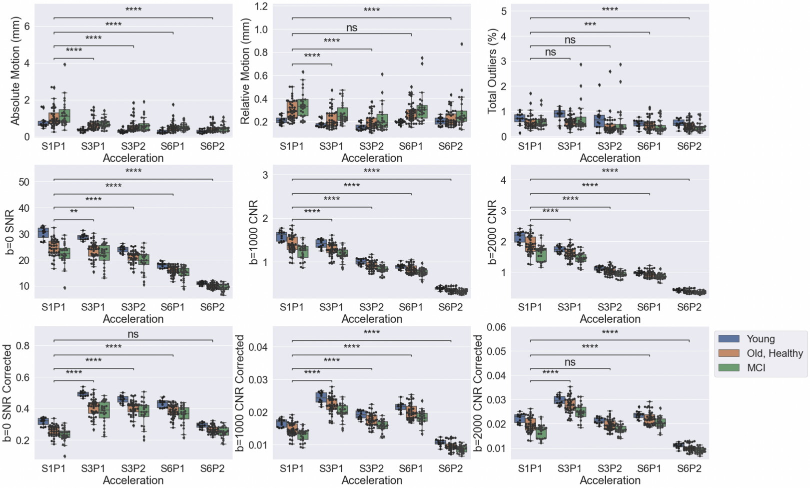


**Figure 2.** Boxplots representing quality control metrics (described on y-axis labels) over different acceleration schemes (x-axis). Blue bars indicate young subjects, orange indicates healthy, old subjects, and green indicates MCI subjects. p-values calculated using a Generalized Estimating Equation (GEE) with Gaussian assumption and exchangeable correlation accounting for repeated subject scans. p-values reported after Bonferroni correction; significance: *p<0.05, **p<0.01,***p<0.001, ****p<0.0001.

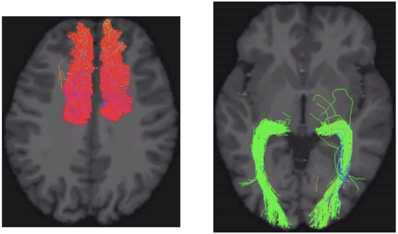

Figure: Example streamlines in frontal (left) and occipital (right) regions. Frontal tracts comprise the anterior cingulate tracts, while occipital tracts the visual pathway from the thalamus to occipital cortex.

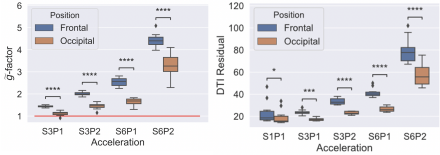


**Figure 3**. Left panel: Average $\tilde{g}$-factor values right panel: Average DTI residual in frontal (blue) and occipital (orange) areas. *p<0.05, ****p<0.001. Red line in left panel indicates $\tilde{g}$-factor of 1, indicating no noise amplification.

Figure: Preliminary results. Noise amplification higher in frontal cortex than occipital.

# Preliminary results

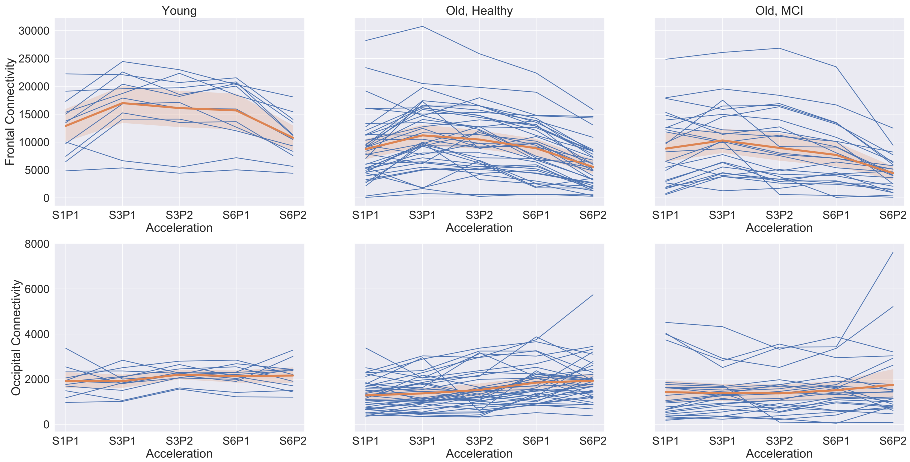


Figure: Initial results suggest streamline counts may somewhat decrease across acceleration factors in frontal regions but are relatively stable for occipital.

## Part 4: Rs-fMRI Data Availability and Open Questions

# OpenNeuro

- 32 subjects (286 rs-fMRI scans, 92 gb) from the Emory Multiband Study are available on OpenNeuro: https://openneuro.org/datasets/ds003540
- Thank you to Raphiel Murden for help with formatting these data in the BIDS data structure.
- Risk et al. (2021) is open access: https://doi.org/10.1016/j.neuroimage.2021.117965

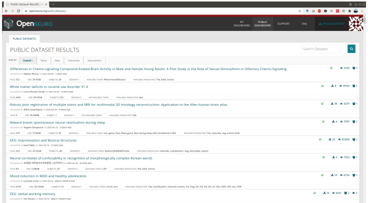

# Open Questions: Other preprocessing pipelines?

Question: What are the impacts in other preprocessing pipelines?

- Ciric et al. (2017) evaluated 14 confound regression methods
- Some require a lot of parameters: 9 regressors, their derivatives, quadratic terms, and squares of derivative = 36 p.
- Popular approach not evaluated here: aCompCor using 10 PCs from regions of no interest Muschelli et al. (2014).
- Scrubbing Power et al. (2012); Ciric et al. (2017): remove data in which the displacement from the previous frame exceeds threshold, e.g., $> 0.25\ mm$.
- Scrubbing based on TR=3 sec.
- With less time between volumes, FD criteria may need to change. (A motion of $> 0.25mm$ across 3 seconds no longer removed.)
- Need new standards for multiband?

# Open Questions: ICA increase benefits?

Question: Can we increase the benefits of MB with ICA artifact removal?

- Easier to remove artifacts in multiband.
- Can we get "better" signal due to ability to unalias respiration, cardiac, CSF pulsation signal from the neural signal?
- Independent component analysis can be used to identify artifacts.
- We also evaluated ICA-AROMA (Pruim et al., 2015) (results not presented or published).
- ICA-AROMA automatically identifies and removes "motion artifacts." We found it also removes a lot of signal.
- ICA-FIX another method (Griffanti et al., 2016).
- ICA-FIX requires more input. May need to train separately for each multiband factor and/or manually classify components.

# Open Questions: Information at higher TR?

Question: Additional information at high temporal resolution?

- Data on the same subjects at different temporal resolutions.
- MB 12: fastest 2-mm publicly available data. 0.512 s between acquisitions. (PNC: 3 seconds, HCP: 0.72 s).
- Is there any more information?
- BOLD is slow. 0.009-0.08 Hz: period is 111 to 12.5 seconds.
- May be information in higher frequency content Feinberg et al. (2010); Lee et al. (2013); Jahanian et al. (2019).
- Spectral analyses: create fconn matrices for different spectral bands; look at coherence.
- Better for dynamic connectivity?

# Examples of processing scripts

- Example processing scripts from the Brain Research in Imaging Statistics Kit: https://github.com/thebrisklab.
- Examples using the `sed` stream editor command for bash.
- Automate creation of preprocessing scripts for each subject.

1. https://github.com/thebrisklab/RestingStateMultiband/blob/main/preprocessing_loopSubjects.sh
2. https://github.com/thebrisklab/RestingStateMultiband/blob/main/preprocessing_singlesubj_3dTproject.sh

# Last slide

- Thank you for listening!
- Please attend SMI 2021!
  https://scholarblogs.emory.edu/smi2021/registration/
- Please submit posters!
  Commit to poster: title and abstract due **April 30th, 2021**. Final poster due **May 9th, 2021**. Email Dr. Suprateek Kundu (suprateek [dot] kundu [at] emory [dot] edu) with questions.
- Also, please vote in the Imaging Section ASA elections!
  https://www.amstat.org/

# References I


Ciric, R., Wolf, D. H., Power, J. D., Roalf, D. R., Baum, G. L., Ruparel, K., Shinohara, R. T., Elliott, M. A., Eickhoff, S. B., Davatzikos, C., Gur, R. C., Gur, R. E., Bassett, D. S., and Satterthwaite, T. D. (2017). Benchmarking of participant-level confound regression strategies for the control of motion artifact in studies of functional connectivity. *NeuroImage*, 154:174–187.

Feinberg, D. A., Moeller, S., Smith, S. M., Auerbach, E., Ramanna, S., Glasser, M. F., Miller, K. L., Ugurbil, K., and Yacoub, E. (2010). Multiplexed echo planar imaging for sub-second whole brain {fMRI} and fast diffusion imaging. *PloS one*, 5(12):e15710.

Griffanti, L., Douaud, G., Bijsterbosh, J., Evangelisti, S., Alfaro-Almagro, F., Glasser, M. F., Duff, E. P., Fitzgibbon, S., Westphal, R., Carone, D., and others (2016). Hand classification of fMRI ICA noise components. *NeuroImage*.

# References II


Jahanian, H., Holdsworth, S., Christen, T., Wu, H., Zhu, K., Kerr, A. B., Middione, M. J., Dougherty, R. F., Moseley, M., and Zaharchuk, G. (2019). Advantages of short repetition time resting-state functional MRI enabled by simultaneous multi-slice imaging. *Journal of Neuroscience Methods*, 311:122–132.

Lee, H. L., Zahneisen, B., Hugger, T., LeVan, P., and Hennig, J. (2013). Tracking dynamic resting-state networks at higher frequencies using MR-encephalography. *NeuroImage*, 65:216–222.

Lindquist, M. A., Geuter, S., Wager, T. D., and Caffo, B. S. (2019). Modular preprocessing pipelines can reintroduce artifacts into fMRI data. *Human Brain Mapping*, 40(8):2358–2376.

Muschelli, J., Nebel, M. B., Caffo, B. S., Barber, A. D., Pekar, J. J., and Mostofsky, S. H. (2014). Reduction of motion-related artifacts in resting state fMRI using aCompCor. *NeuroImage*, 96:22–35.

Power, J. D., Barnes, K. A., Snyder, A. Z., Schlaggar, B. L., and Petersen, S. E. (2012). Spurious but systematic correlations in functional connectivity MRI networks arise from subject motion. *NeuroImage*, 59(3):2142–2154.

# References III


Pruim, R. H., Mennes, M., van Rooij, D., Llera, A., Buitelaar, J. K., and Beckmann, C. F. (2015). ICA-AROMA: A robust ICA-based strategy for removing motion artifacts from fMRI data. *NeuroImage*, 112:267–277.

Risk, B. B., Murden, R. J., Wu, J., Nebel, M. B., Venkataraman, A., Zhang, Z., and Qiu, D. (2021). Which multiband factor should you choose for your resting-state fMRI study? *NeuroImage*, 234:117965.

Setsompop, K., Gagoski, B. A., Polimeni, J. R., Witzel, T., Wedeen, V. J., and Wald, L. L. (2012). Blipped-controlled aliasing in parallel imaging for simultaneous multislice echo planar imaging with reduced g-factor penalty. *Magnetic Resonance in Medicine*, 67(5):1210–1224.